

Uniwersytet Wrocławski
Wydział Nauk Biologicznych

Monika Krzyżanowska

numer albumu: 270882

Praca Magisterska

**Wpływ tkankowo-specyficznego wyciszenia ekspresji
białka Hsp67Bc u *Drosophila melanogaster***

Effects of tissue-specific knockdown of Hsp67Bc in *Drosophila melanogaster*

Praca wykonana pod kierunkiem Pani dr Magdy Dubińskiej-Magiery

W Instytucie Biologii Eksperimentalnej

W Zakładzie Biologii Rozwoju Zwierząt

Wrocław, 2019

TABLE OF CONTENTS

Chapter 1: ABBREVIATIONS.....	4
Chapter 2: SOURCES OF PICTURES.....	5
Chapter 3: INTRODUCTION.....	6
3.1 Aim of the thesis.....	6
3.2 Objectives and questions.....	6
3.3 Literature review.....	7
3.3.1 Small heat shock proteins family.....	7
3.3.2 Mammalian ortholog of Hsp67Bc – HSPB8.....	8
3.3.3 Hsp67Bc – an introduction.....	10
Chapter 4: MATERIALS AND METHODS.....	13
4.1 Research methodology and hypotheses.....	13
4.2 Drosophila husbandry.....	14
4.3 Behavioral tests methodology.....	14
4.4 Statistical analysis and data visualization.....	15
4.5 Contractility tests.....	16
4.5.1 Larval somatic muscle dissection and preparation.....	16
4.5.2 Microscopy.....	17
4.5.3 Image and data processing.....	17
4.6 Morphometric characterization of neuromuscular junctions (NMJ).....	18
4.6.1 Larval somatic muscle dissection and preparation.....	18
4.6.2 Microscopy.....	19
4.6.3 Image and data processing.....	19
4.7 Oxyblot TM with body wall muscles.....	19
4.7.1 Sample preparation.....	19
4.7.2 Derivatization and immunoblotting.....	21
Chapter 5: RESULTS.....	22
5.1 Effects of muscle-specific Hsp67Bc silencing.....	22
5.1.1 Muscle-specific Hsp67Bc silencing alters muscle structure.....	22
5.1.2 Muscle specific Hsp67Bc silencing changes larvas behavior.....	23
5.1.3 Muscle-specific Hsp67Bc silencing does not affect muscle contractility.....	24
5.1.4 Muscle-specific Hsp67Bc silencing increases the level of muscle protein oxidation.....	25
5.2 Evaluation of neuronal-specific Hsp67Bc silencing.....	26
5.2.1 Neuronal-specific Hsp67Bc silencing alters NMJ structure.....	26
5.2.2 Neuronal-specific Hsp67Bc silencing alters larvas behavior in righting and crawling assay.....	28
Chapter 6: DISCUSSION.....	29
Chapter 7: ACKNOWLEDGMENTS.....	35
Chapter 8: LITERATURE.....	36
Chapter 9: ABSTRACT.....	39
9.1 Streszczenie w języku polskim (abstract in Polish language).....	39
9.2 Abstract in English language.....	39

CHAPTER 1: ABBREVIATIONS

ABS – Absorbance

ALS – Amyotrophic Lateral Sclerosis

BCA – Bicinchoninic Acid

BSA – Bovine Serum Albumin

CI – Contractility index

CMAP – Compound muscle action potential

CMT – Charcot-Marie-Tooth

DAPI – 4,6-diamidino-2-phenylindole

dHMN – Distal Hereditary Motor Neuropathy

DTT – Dithiothreitol

HSP – Heat shock protein

IQR – Interquartile range

NMJ – Neuromuscular junctions

PBST – Phosphate buffer saline with Tween 20

PCR – Polymerase chain reaction

PFA – Paraformaldehyde

PMSF – Phenylmethylsulfonyl fluoride

RNA-Seq – RNA sequencing

RT-PCR -- Real time polymerase chain reaction

sHSP – Small heat shock protein

UAS – Upstream activation sequence

WT – Wild Type

CHAPTER 2: SOURCES OF PICTURES

Figure 1: <http://flybase.org/reports/FBgn0001229> (access in May 2019)

Figure 2: based on the data from: <http://flyatlas.gla.ac.uk/FlyAtlas2/index.html?search=gene&gene=CG4190&idtype=cgnum#mobileTargetG> (access in May 2019)

Figure 3: from own sources

Figure 4: from own sources

Figure 5: from own sources

Figure 6: based on photographs taken by Ph.D. Magda-Dubińska Magiera

Figure 7: from own sources

Figure 8: from own sources

Figure 10: from own sources

Figure 9: from own sources

Figure 11: from own sources

Figure 12: from own sources

Figure 13: based on photographs taken by Ph.D. Magda-Dubińska Magiera

Figure 14: from own sources

CHAPTER 3: INTRODUCTION

3.1 Aim of the thesis

In this thesis the author examined the effect of tissue-specific knockdown of Hsp67Bc protein expression by RNAi in *Drosophila melanogaster*.

The reason to choose this subject was to expand knowledge about Hsp67Bc, which is a member of the family of small heat shock proteins. Hsp67Bc has human functional ortholog which is a potential target of treatment therapy for many diseases. This thesis is a continuation of research concerning small heat shock proteins conducted in the Department of Animal Developmental Biology, University of Wroclaw.

The choice of the subject was also influenced by the interests of the author in animal development, genetic engineering and research techniques which were used in the study.

3.2 Objectives and questions

The main research question is: **Does tissue-specific silencing of Hsp67Bc gene alter the structure and function of muscle and nerve in *Drosophila melanogaster* 3rd instar larvae?** The main hypothesis assumes that tissue-specific Hsp67Bc gene expression knock-down alters muscle and nerve system structure and function. The main objective of the thesis is to answer the research question.

The workflow of the thesis contains particular steps:

- performing a series of experiments and collect data,
- data visualization and statistical analysis (chapter Chapter 5: RESULTS),
- discussion (Chapter 6: DISCUSSION).

3.3 Literature review

3.3.1 Small heat shock proteins family

sHsp family is the group of conservative protein with similar structure, locus and function, existing in all living organisms including humans. The sHSPs are characterised by low molecular mass (15-42 kDa). This group of proteins displays chaperone functions¹. A number of sHSP differs among organisms. sHsps' expression is different depending on cell type and environmental conditions. Their name "heat shock" indicates participation in heat shock response but actually, sHSPs, in general, are involved in response to different stress conditions and maintaining of cell homeostasis, and not all of them participate in heat shock response [10].

Each cell of the organism has to deal with a toxic accumulation of oxidized, misfolded protein. The effectivity of dealing with stress conditions decreases during aging [22]. sHSPs protect the cell against toxic protein aggregation in a crowded cellular environment. sHSPs protect the cell against damage via assisting in refolding of stress-denatured proteins and creating networks of protein quality control. Nonfunctional sHSPs lead to many diseases [32].

In literature names of sHSP family members often derive from its molecular weight in kDa however this rule is not used by all researchers. Different names for the same proteins exist in literature which can lead to misunderstanding. There is an example herein: human ortholog of fly Hsp67Bc is named HSPB8 and Hsp22. Simultaneously among *Drosophila melanogaster* sHSP family also exists Hsp22 protein, which is not an ortholog of human HSPB8/Hsp22. The solution to all doubts is to search for information about proteins in databases (example popular database: <https://www.ncbi.nlm.nih.gov/>).

sHSPs have varied functions in muscle tissues both skeletal and cardiac. Seven sHSPs were localized in skeletal muscle tissue: HSPB1, HSPB2, HSPB3, HSPB5, HSPB6, HSPB7 and HSPB8. One of them: HSPB1 is responsible for protecting muscle cells against oxidative stress [8]. Some studies suggest that sHSPs are expressed at higher levels in muscle tissue during exercise, protecting against oxidative stress and heat [20].

1 Chaperones are proteins that assist in folding and unfolding of another molecular structures.

sHSPs participate in organism development in *D. melanogaster* and create an individual pattern of expression in specific cells and tissues induced by heat-shock [18].

3.3.2 Mammalian ortholog of Hsp67Bc – HSPB8

Hsp67Bc was identified as the closest ortholog of human HSPB8 protein because of the same functions demonstrated *in vitro* [4]. HSPB8 is also known as HSP22, because of 22 kDa weight. Its expression is dependent on many unknown factors. HSPB8 takes part in cell protection against unfolded or misfolded proteins regulating its proteolytic degradation [21]

HSPB8 creates dimers but there is evidence of its existing in the cell as a monomer. This protein is involved in interactions with another sHSPs, such as HSPB1, HSPB2 and HSPB7 [29].

Hot-spot mutations in human HSPB8 cause human neurodegenerative diseases (CMT 2L (Charcot-Marie-Tooth type 2) and dHMN (distal hereditary motor neuropathy)) which cause muscle atrophy and often lead to disability [11]. As potential disease treatment target HSPB8 is highly studied. Knowledge about HSPB8 mutations allows to precise patient's diagnosis but nowadays there is no cure for diseases mentioned above. Research on hot-spot mutated HSPB8 protein and its orthologs allows to better understand disease mechanisms. Studies on HSPB8 were performed on model organisms and *in vitro* human cell cultures [16].

HSPB8 is related to more neurodegenerative diseases with various pathological mechanisms such as Parkinson's disease, Alzheimer's disease, Huntington's disease and spinocerebellar ataxia type 3. In all of them, HSPB8 protects against protein aggregations or degrades misfolded proteins in interactions with other proteins. HSPB8 as protein related to neurodegenerative diseases is a potential target of treatment. Aggregates found in mentioned diseases are amyloids which are highly insoluble [31].

HSPB8 is involved in heart growth mechanism in mammals. Tissue-specific overexpression of human HSPB8 in transgenic mice leads to heart hypertrophy (30% increased) *in vivo*. Moreover, culture *in vitro* studies on rat neonatal cardiac myocytes

show cell hypertrophy and increased mRNA expression of fetal genes usually up-regulated during heart hypertrophy [6]².

Another study shows that HSPB8 knock-out in mice is related to heart failure during cardiac overload [27].

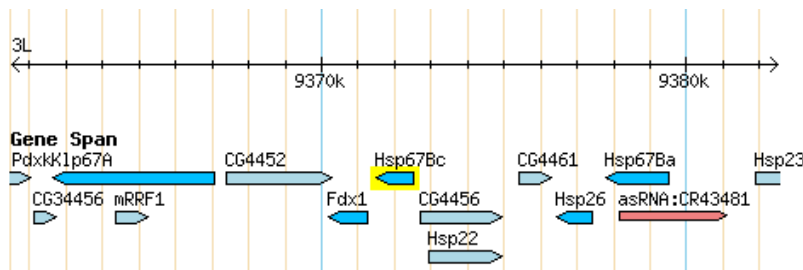
Other studies on HSPB8 on mice were performed: knock-out of HSPB8 and knock-in of 141N hot spot mutation (which is responsible for Charcot-Marie-Tooth disease in human). 141N knock-in leaded to significant impairment of behavioral and electrophysiological studies resulted in drastically altered locomotor performance and the Compound Muscle Action Potential (CMAP) amplitude. There were observed histopathological changes in nerve ultrastructure such as severe axonal degeneration, degenerating organelles, regenerative clusters and onion bulb formations. Muscles were also affected which was visible in muscle ultrastructure (altered Z-bands and small, empty vacuoles) and structure (discrepancy in myofiber sizes and atrophic myofibers). Changes were observed in older mice and absent in younger mice which suggest that all symptoms related to 141N mutation are progressive degeneration, not developmental impairment. Pathologic phenotype presented in HSPB8 141N knock-in mice is similar to CMT human phenotype.

Knock-out of mouse HSPB8 does not alter muscle function in behavioral and physiological tests (average strength, time on the rotor and CMAP amplitude). It suggests that HSPB8 loss of function in mice does not lead to myopathic/neuropathic changes, however 12-month-old mouse's skeletal muscles' ultrastructure were altered (enlarged, altered and undergoing mitophagy mitochondria with degenerating cristae and abnormal matrix) [3].

2 In this publication HSPB8 is named as H11 kinase – rarely used name of this protein, existing in ncbi protein database: <https://www.ncbi.nlm.nih.gov/protein/AAP35522.1>.

3.3.3 Hsp67Bc – an introduction

Hsp67Bc is also known as gene 3 or CG4190. It is localized in 67B locus in fruit fly genome, where are genes coding for sHSP family (Fig. 1) All sHSPs from this locus (Hsp67Bc, Hsp22, Hsp23, Hsp26 and Hsp27) have similar structure, containing 83-aminoacid fragment, conservative to mammal chain B2 from Alfa-Crystalline protein [2].



Hsp67Bc does not contain any intron and its expression is induced by heat shock [25].

Figure 1: **Gene map of Hsp67Bc locus.**

gene expression depends on the developmental stage and tissue. Hsp67Bc is expressed during development: embryogenesis and pupation [25].

In vivo studies on *Drosophila melanogaster* show that Hsp67Bc prevents protein aggregation in Hsp70 independent pathway in the most efficient way among other sHSPs. It is heat-inducible protein, the same as Hsp22, Hsp23, Hsp26, Hsp27, HspBa, L(2)efl, CG4461 and Hsp70Aa. Hsp67Bc does not participate in protein refolding. Hsp67Bc with another sHSP protein: CG14207 both prevent aging. Their overexpression is related to longer lifespan [32]

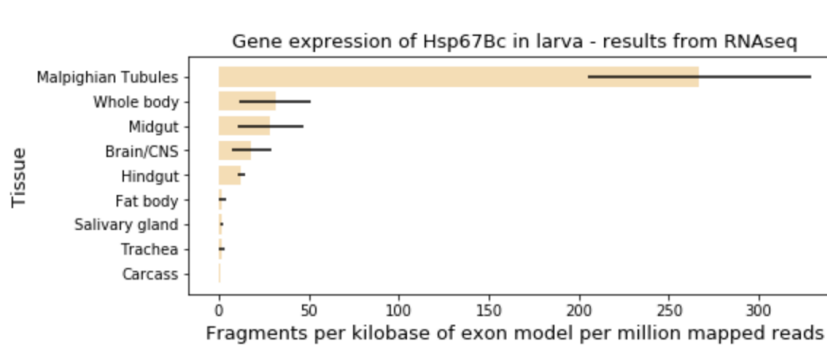


Figure 2: **Hsp67Bc expression in few selected organs in larva.** Results from RNAseq. Errorbars +-SD (<https://flybase.org>).

Larva tissues differ in the level of Hsp67Bc mRNA expression. The highest expression was observed in malpighian tubules (using RNA-seq

data from <https://flybase.org>) among other, following organs: brain, salivary glands, trachea, hindgut, fat body, midgut, carcass and whole body (Fig. 2) This data do not include all organs.

Hsp67Bc knock-down using actin-GAL4/UAS-RNAi alters fly's wings and bristles morphology. Bristle is related to central nervous system development thus these studies suggest an important role of Hsp67Bc in nerve system development [30].

The Hsp67Bc sequence contains hot-spot which seems to be analogical to HSPB8 hot spot, responsible for diseases mentioned above. Tissue-specific overexpression of Hsp67Bc with mutation 126K→E and 126 K→N in *D. melanogaster* larvae leads to symptoms similar to the mammalian phenotype of neurodegenerative diseases. Each substitution leads to another impact on muscle function and structure both in human HSPB8 and *D. melanogaster* Hsp67Bc [14].

Hsp67Bc was identified as human HSPB8 ortholog because of its role in autophagy induction via pathway related to eIF2-alpha. Hsp67Bc also protects the cell against mutated proteins: ortholog of human HSPB1 and ataxin-3. Despite low sequence homology between *D. melanogaster* Starvin and human BAG3 *D. melanogaster* Hsp67Bc interacts both with Starvin and human BAG3 in co-immunoprecipitation. Hsp67Bc the same as HSPB8 inhibit eye degeneration caused by mutated polyglutamine [4].

There are other studies confirming Hsp67Bc as an ortholog of HSPB8. Amyotrophic lateral sclerosis (ALS) is a neurodegenerative disease, caused by the accumulation of toxic aggregates of TAR-DNA-binding proteins (TDP-34, TDP-25, and TDP-35). HSPB8 enables degradation of these aggregates. Its overexpression in immortalized motor neurons reduce accumulation of TDP proteins. The same effect was observed in transgenic *D. melanogaster* with an eye-specific expression of mutated human TDP-43-NLS. Flies with mutated TDP-43-NLS have progressive eye degeneration which was reduced with Hsp67Bc overexpression. Additionally Hsp67Bc downregulation increases aggregation of toxic TDP-43-NLS [5].

There are also discoveries about upregulation of Hsp67Bc mRNA expression in the wing imaginal disc by Pacman 5'-3' exoribonuclease. Level of gene expression was studied using RT-PCR and microarrays. When Pacman is mutated Hsp67Bc gene

expression is 2.5 fold higher. This suggests that Pacman regulates expression of Hsp67Bc [15].

Literature review shows Hsp67Bc as the closest functional ortholog of human HSPB8, participating in biological mechanisms analogical to human HSPB8. Hsp67Bc interacts *in vivo* as well as *in vitro* with proteins that have their own human orthologs. *D. melanogaster* is good animal model of diseases related to HSPB8 protein.

CHAPTER 4: MATERIALS AND METHODS

4.1 Research methodology and hypotheses

To answer research question series of experiment were performed. Chosen methods and questions were based on literature and previous discoveries and were established before start of the work. Chapter 4: MATERIALS AND METHODS contains a detailed description of performed experiments, which allows repeating these experiments by another researcher.

All experiments were performed on third instar larvae, because of the simplicity of this model and well-described methodology.

The experiments were performed using the GAL4/ UAS system which is a method of activating gene expression in *Drosophila melanogaster*. The GAL4 is the transcriptional activator in this system. The upstream activation sequence (UAS) is an enhancer that is specific to the GAL4 protein. All experiments were divided into two groups and each group involved different driver lines. The goal was to receive offspring of larvae with tissue-specific RNAi sequence expression. Parents were: virgin females which had driver gene and males which have gene coding RNAi sequence specific to gene of interests (Hsp67Bc). Tissue-specific gene silencing in offspring is a result of a composition of two components described above: driver gene and RNAi sequence. The Gal4/UAS method used in this study allows to control the experiment.

Each particular experiment was performed on a test group (RNAi line) and control group (driver line). Comparison of the results obtained from experiments between the test group and the control group will lead to answer the research question.

Behavioral test (crawling and righting) were performed on both crosses. The hypothesis is that Hsp67Bc gene silencing alters larvae behavior in comparison to the control group.

Offspring of mefxCG4190 cross has Hsp67Bc interference in heart and somatic muscles. Dissected body wall muscles were used as material to perform **contractility tests** and **assessment of body wall muscle morphology**.

Offspring of elavxCG4190 cross have interference in the nervous system, which includes brain and body nerves. **Morphometric measurement of neuromuscular junctions** (NMJ) allows observing morphological changes in NMJ and answer hypothesis that Hsp67Bc expression interference alters neuromuscular junctions structure.

Oxyblot were performed on muscles dissected from mefxCG4190 cross. Oxyblot allows answering to the hypothesis that Hsp67Bc gene silencing alters the level of protein oxidation in body wall muscle tissue.

4.2 Drosophila husbandry

Fly stocks were maintained on the standard agar-meal corn media To drive gene expression to target tissues GAL4-UAS system was used. Tissue-specific expression in muscles was targeted by the *mef2-GAL4* driver (Bloomington Drosophila stock center) and in neurons was targeted by *Elav-GAL4* (Bloomington Drosophila stock center). Driver lines were crossed with CG4190 (VDRC stock center: Hsp67BcRNAi-UAS (26416). Crosses were maintained at 25°C. Anesthesia of flies to virgins and males collection was performed using on flypad with CO².

4.3 Behavioral tests methodology

Behavioral tests were performed under a stereoscopic microscope on the petri dish with 1% apple juice agar medium³, prepared under the laminar. Petri dish with juice can be stored up to 2 weeks in the fridge. Underneath Petri dish millimeter paper with x, y coordinates to measure larva's movement distance was placed (Fig. 3 A). Each measurement was repeated 3 times on each larva from the least stressful (crawling) to the most stressful (righting) experiment. Each larva was placed using the brush in the middle of Petri dish (in the 0,0 coordinates in millimeter paper) and have some time to adapt to a new environment (between 10-30 seconds, until larva started to crawl). Crawling assay was performed 30 seconds and following data were collected: number of peristaltic movements, number of reorientation points, anterior part's position on

³ 2% concentration of agar is better (allows to avoid scratches on medium surface), but 1% was used to continue procedure in the same condition as was begun. Scratches on surface draw larvas attention and disrupt crawling behavior (measurement have to be repeated).

coordinates in the start and end of the measurement (crawling distance was calculated using these points with Pythagorean theorem formula) (Fig. 3). After crawling measurement millimeter paper was moved to have (0,0) point under larva's anterior part

to perform next repetition. After 3 repetitions of crawling assay righting assay was performed also 3 times. Each larva was inverted to dorsal position and time to come back to the ventral position was counted. Behavioral tests were performed 3 times (each on a different day) on 15 larvae. In summary 45 larvae was measured.

The methodology was designed regarding methods described in [14], [33] modified and expanded to own methods to detect more larvae behavior variants during crawling (reorientation points and distance), described in [9].

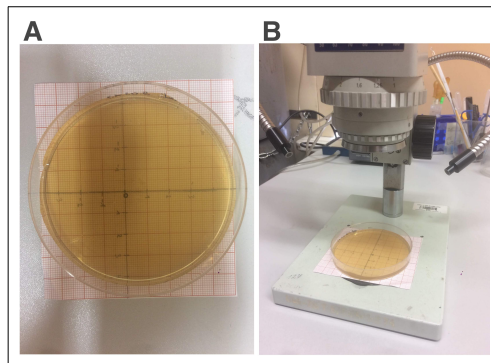
Figure 3: Behavioral tests methodology.

(A) Petri dish with 1% apple juice-agar and millimeter paper underneath with x, y coordinates (B) placed under stereoscopic microscope.

Environmental factors such as air temperature, humidity, intensity of light, temperature of the agar medium, date of preparing agar medium and another factors that are not known can change results of the experiment. Therefore 3 experiments were performed in separate days on different crosses. If the availability of material allowed, larvae were measured in turns (one larva from RNAi expressing line, one larva from control) with careful attention to not confuse lines.

4.4 Statistical analysis and data visualization

Statistical analysis was performed in Jupyter Notebook in Python 3.7 programming language. Data was organized and stored in LibreOffice (Version: 6.2.1.2) spreadsheet and converted to a csv file. Statistical tests and data visualization were performed using following packages (versions in brackets): seaborn (0.9.0), scipy (1.1.0), pandas (0.23.4), numpy (1.15.4), matplotlib (3.0.2). Jupyter notebooks with analysis and data in csv files are available in GitHub repository (please contact author to access) with additional plots, which weren't included herein.



Statistical significance was calculated using parametric t-test (`scipy.ttest_ind()` function) for data with normal distributions and non-parametric Spearman test (`scipy.spearmanr()` function) for data with not normal distribution and small sample size (in the Oxyblot experiment).

Box plots. Boxes represent interquartile range (IQR) with median inside. Lower whiskers indicate $Q1 - 1.5 \times IQR$ and upper whiskers indicate $Q3 + 1.5 \times IQR$. Statistical significance based on P-value was marked on plots respectively: ns - $P > 0.05$, * - $P \leq 0.05$, ** - $P \leq 0.01$, *** - $P \leq 0.001$, **** - $P \leq 0.0001$.

Histograms. A number of bins were created automatically according to Freedman–Diaconis rule with kde estimation.

4.5 Contractility tests

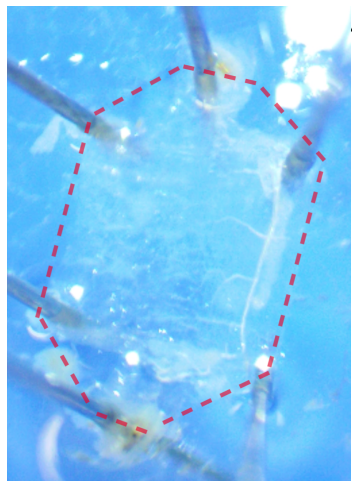


Figure 4: Larval somatic body wall muscles dissection on silicon plate.
The muscles are marked with a dotted, red line around.

4.5.1 Larval somatic muscle dissection and preparation

- 1 The muscle was dissected in silicon plate using 0,2 mm needles under a stereoscopic microscope (Fig. 4) and divided into 2 groups:
 - Dissection in 25 mM EDTA and 125 mM NaCl to receive relaxed muscle fibers,
 - Dissection in 125 mM NaCl, without EDTA to receive contracted muscle fibers,
- 2 After dissection muscles were fixed in 4% PFA 20-30 minutes.
- 3 Fixed muscles were transferred to 2 ml Eppendorf tube and rinsed 3 times for 5 minutes in 0.5% PBST (19 mM NaH₂PO₄, 8 mM Na₂HPO₄, 145mM NaCl, 0.5% Tween 20) on a 3D rotator.
- 4 Staining was performed 10 minutes using 0,2 µg/ml DAPI (1:10000) and Alexa 546 (1:80) diluted in 0.5% PBST on the 3D rotator.

- 5 Muscles were rinsed 3 times for 15 minutes in 0.5% PBST on the 3D rotator.
- 6 Muscles were mounted in fluorescent mounting medium (Dako) on standard microscope slides.

4.5.2 Microscopy

For imaging, Olympus FluoView FV1000 confocal laser scanning microscope (Olympus) was used. The images were recorded by employing Plan-Apochromat 20x and 40x objectives.

4.5.3 Image and data processing

The model muscles used to this experiment were ventral longitudinal VL4 and VL3 and all comparisons were made using images of these muscles. From each individual was collected between 1-5 images from different body wall muscle segment (dependent on the quality of preparation). The muscle was measured in FIJI software in pixels, recalculated to μm , depending on the scale. Data was collected in LibreOffice (Version: 6.2.1.2) spreadsheet.

Before performing described below CI (Contractility index) calculation statistical significance of the difference between relaxed fibers and contracted fibers were calculated using a t-test, and data was visualized on the plot.

CI calculation was performed using 2 methods: based on the formula described in [14] ($\text{CI} = (\text{size of relaxed fibers} - \text{size of contracted fibers})/\text{size of relaxed fibers}$) and its modification.

First method bases on CI calculated from the mean and median of all relaxed/contracted muscles. Result of this method is one number – mean or median contractility index.

The second method is *in silico* simulation using an algorithm written in Python 3.7 programming language. Simulation performs a given number of iterations (herein – 1000 iterations). Each iteration matches all muscles from the dataset in pairs (relaxed + contracted), calculates CI from each pair and calculates mean CI from all 1000 iterations. Iterations with negative CI number (in combination when the relaxed muscle

is shorter than contracted) were excluded. Diversity of muscle sizes between individuals and segments can disrupt CI calculation, because sometimes relaxed muscle is shorter than contracted muscle. Exclusion of negative CI applies the test to muscle length diversity among individuals.

Images prepared for contractility tests were used also to the morphological characterization of the muscle fiber.

4.6 Morphometric characterization of neuromuscular junctions (NMJ)

4.6.1 Larval somatic muscle dissection and preparation

1. The muscle was dissected in silicon plate using 0,2 mm needles in under stereoscopic microscope in 25 mM EDTA and 125 mM NaCl,
2. After dissection muscles were fixed in 4% PFA 20-30 minutes.
3. Fixed muscles were transferred to 2 ml Eppendorf tube and rinsed 3 times for 5 minutes in 0.5% PBST on a 3D rotator.
4. Muscles were blocked for 1-2 hours in blocking solution (horse serum in 0,5% PBST) on 3D rotator.
5. Muscles were incubated overnight with primary antibody (Anty-Brp⁴, mouse monoclonal (4F3, DSHB)) diluted 1:200 in 0,5% PBST at 4°C.
6. Fixed muscles were rinsed 3 times for 5 minutes in 0.5% PBST on the 3D rotator.
7. Muscles were incubated 1hour with secondary antibody goat anti-mouse IgG conjugated to CY5 (Jackson ImmunoResearch) in 0.5% PBST.
8. Staining was performed 10 minutes using 0,2 µg/ml DAPI (1:10000) and Alexa 488-conjugated phalloidin was used (at a concentration of 2 µg/ml; Life Technologies) (1:100) diluted in 0.5% PBST on lab rotator.
9. Muscles were rinsed 3 times for 15 minutes in 0.5% PBST on lab rotator.

4 Anty-Brp antibody specifically labels presynaptic zones.

10. Muscles were mounted in fluorescent mounting medium (Dako) in standard microscope slides.

4.6.2 Microscopy

Procedure described in chapter 4.5.2.

4.6.3 Image and data processing

The model muscle used to this experiment was lateral longitudinal LL1 (surface area) used for all comparisons in this experiment. From each individual was collected between 1-5 images from different body wall muscle segment (dependent on the quality of preparation). The buttons were measured in the FIJI software in pixels, recalculated to μm , depending on the scale. Buttons had an elliptical shape thus radii values are in real semi-minor axes of the ellipses. Usually, semi-minor axes of the buttons were in a perpendicular orientation to the “chain” created by NMJs. Data was collected in LibreOffice (Version: 6.2.1.2) spreadsheet.

4.7 OxyblotTM with body wall muscles

OxyblotTM is a research technique which allows detecting the level of protein oxidation using immunodetection of carbonyl groups. The experiment was performed according to the following steps: preparation of protein lysates, derivatization, SDS-page, transfer and immunodetection.

4.7.1 Sample preparation

1. Body wall muscles dissection

Muscles were dissected on silicon plate using dissection needles and stored in -80°C in Eppendorf tube. This dissection procedure is different than previously described dissection to microscopy (chapters: 4.5.1, 4.6.1) because doesn't require cutting through the body wall center, flattening and stretching using 6 needles (as in Fig. 6). Dissection requires the use of one needle punctured in the posterior part, cutting anterior part (with mouth hooks) and removing internal organs.

2. Lysates preparation

All procedures were performed in 4°C. Samples were homogenized in RIPA + 50mM DTT + 1:20 proteases inhibitor (50 µl of solution per 10 body wall muscles) using micro homogenizer. RIPA solution contains: 50mM Tris (pH = 8.0), 150mM NaCl, 0.02% sodium azide, 0.1% SDS, 1.0 % Nonidet P-40, 0.5% sodium deoxycholate, 100 µg/ml PMSF and 1 µg/ml aprotynine). Samples were centrifuged 20 minutes in 12000xg. Supernatants were collected and stored in 4°C up to 1 day.

For control and RNAi line, two muscle lysates from 10 individuals were used (finally 20 individuals per line).

3. Protein concentration measurement

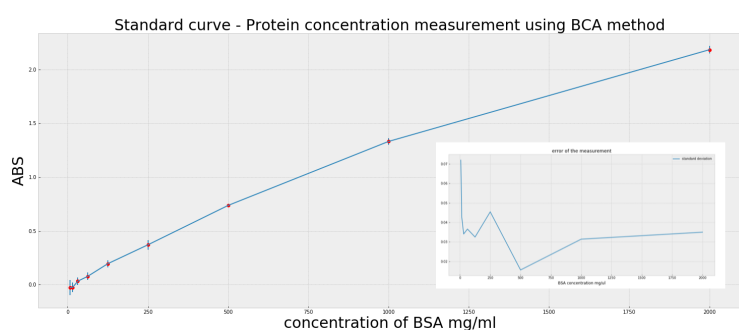


Figure 5: Standard curve of protein concentration.
Error bars indicate standard deviation. N=5.

Protein concentration was measured using Pierce™ BCA Protein Assay Kit (ThermoFisher, cat. 23225) according to enclosed protocol modified to apply in NanoDrop Denovix DS-11.

A standard curve (Fig. 5) was prepared using BSA standard, diluted 2 times in range 7.8 – 2000.0 mg/ml in RIPA + 1mM DTT. The low detection limit was calculated using the methodology described in [1] and is 54 mg/ml. Additionally, all concentrations with negative ABS (absorbance) was excluded, as indistinguishable from blank.

Before measurement samples were diluted 1:50 in RIPA to obtain 1mM DTT concentration (DTT is an inhibitor of BCA reaction, and started 50mM concentration does not allow to measurement).

4.7.2 Derivatization and immunoblotting

From each lysate 4 derivatization reactions were performed, using 20 ng of protein. All samples were divided into 2 polyacrylamide gels, to perform two separated Oxyblots with the same samples.

Derivatization reaction and immunoblotting were performed according to the protocol enclosed to Oxyblot protein oxidation detection Kit (Sigma-Aldrich, cat. S7150). 10 % resolution gel and 6% stacking gel were used to SDS-page and electrophoresis was performed 1:15 h in 100V. The transfer was performed 1:15 h with 400 mA.

1. Quantification

Detection and documentation were made using Bio-rad system. Signal from chemiluminescent detection was normalized to Ponceau staining. Intensity of signal (Integral density) and Area for each particular lane were measured in Fiji software. Oxidation index was calculated for each lysate, using formula:

$$["Ponceau"] = ["Ponceau-density"] / ["Ponceau-area"]$$

$$["Chemiluminescent"] = ["Chemiluminescent-density"] / ["Blot-area"]$$

$$["Oxidation\ index"] = (["Chemiluminescent"] / ["Ponceau"]) * 100$$

["Ponceau"] is density per one pixel for lane (Ponceau staining). ["Chemiluminescent"] is density per one pixel from lane (chemiluminescent immunodetection). Oxidation index is the value that was used to carry out the statistical analysis.

CHAPTER 5: RESULTS

5.1 Effects of muscle-specific Hsp67Bc silencing

5.1.1 Muscle-specific Hsp67Bc silencing alters muscle structure

VL4 and VL3 model muscles of larvae with muscle-specific Hsp67Bc silencing differ from control muscles in two parameters. The disturbances present in Hsp67Bc knockdown muscles stained with phalloidin comprise fuzzy Z-bands and splitted myofibers (Fig. 6A-C). The majority of control muscles has a proper structure, typical for WT muscle (Fig. 6D). However in control, some altered muscles are also present, but in less number. A statistical summary is visualized on the plot (Fig. 6E). In all investigated images splitted myofibers are present 9.5 fold more often in RNAi expressing muscles than in control and fuzzy Z-bands are 12.1 fold more often.

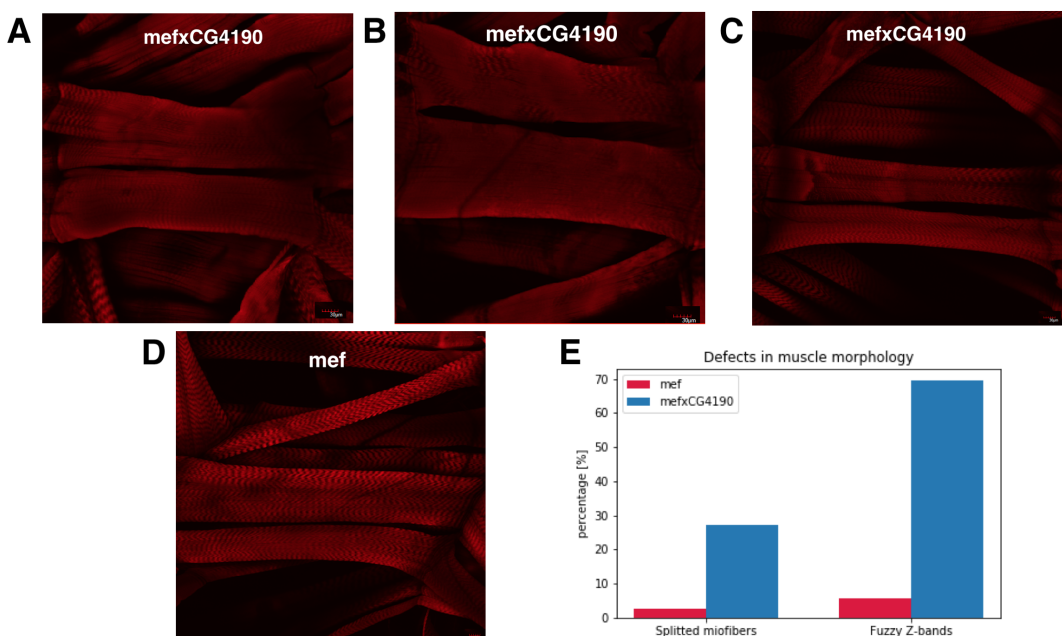


Figure 6: Muscle Morphology in larvae with muscle-specific Hsp67Bc silencing.
Representative view of segments with lateral VL4 and VL3 in the middle stained with phalloidin. (A, B, C) represent mefxCG4190 (RNAi). (D) represents control (mef). (E) shows percentage of splitted myofibers and fuzzy Z-bands in summary among all analyzed images ($n=35$ for mef and $n=33$ for mefxCG4190). Based on photographs taken by Ph.D. Magda-Dubińska Magiera.

5.1.2 Muscle specific Hsp67Bc silencing changes larva behavior

For the experiment with *mef* drivers, two behavior tests were performed. The first was crawling test allowing to assess the number of peristaltic movements per 30 seconds during crawling and second was righting assay. There were no statistically significant differences between control and RNAi line in crawling tests. (Fig. 7A). In righting test time to come back to the normal position was significantly shorter ($P < 0.001$) in the RNAi line (Fig. 7B). There was no correlation between righting and crawling experiment for each individual. (Fig. 7C). Larvae with ability to make righting assay shorter do not make more peristaltic movements. Data distribution in righting for control (E) test shows a small bimodal trend in the right side of the curve for RNAi expressing line.

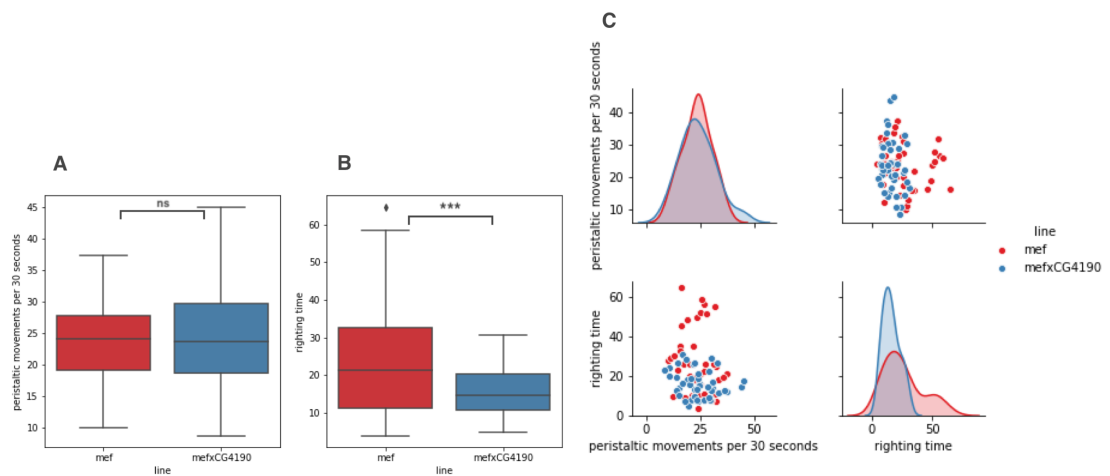


Figure 7: Behavioral tests of larvae with muscle-specific Hsp67Bc silencing.
Results of behavioral tests with 3rd instar larvae using *mef2-Gal4* driver line as control ($n=45$). Each larva was measured 3 times and mean was calculated. (A) Crawling assay – number of peristaltic movements per 30 seconds. (B) Righting assay – time in seconds to come back to normal body position. (C) Correlation between crawling and righting assay for each individual and distribution of the dataset.

5.1.3 Muscle-specific Hsp67Bc silencing does not affect muscle contractility

Before CI calculation t-test was performed to check statistical significance between muscle lengths dissected in buffer with EDTA and without EDTA ($P < 0.001$). A statistically significant difference between relaxed and contracted muscle allows confirming that muscle dissection was performed properly (Fig. 8A).

CI differs between 3 calculation methods used for data analysis (Fig. 8E). CI calculated from mean and median of all muscle lengths is higher in RNAi expressing line in opposite to result from *in silico* simulation. Method using CI calculated from mean and median doesn't allow to calculate standard deviation and statistical significance. The result from *in silico* simulation is statistically insignificant. Additionally there are no statistically significant differences between muscle length between control and RNAi expressing line (Fig. 8B,C).

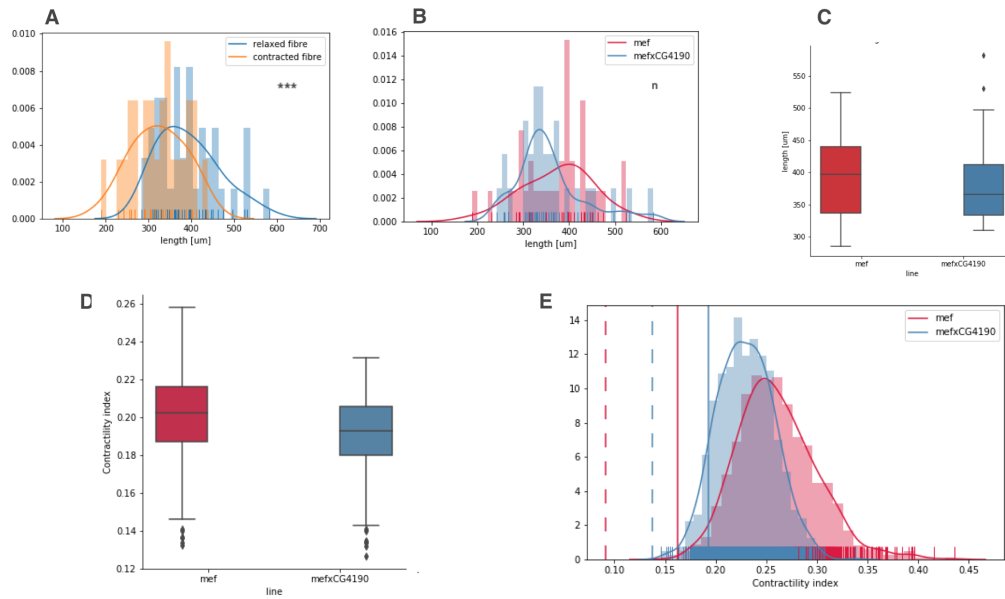


Figure 8: Contractility tests of larvae with muscle-specific Hsp67Bc silencing.
 Results of contractility test with 3rd instar larvae using *mef2-Gal4* driver line as control. Body wall muscles were dissected and measurements were performed on VL4 muscle from different segments of body ($n = 12-23$). (A) Before Contractility index calculation difference between muscles dissected in EDTA (relaxed) and without EDTA (contracted) were calculated ($P < 0.001$). (B) (C) Distribution of the relaxed VL4 muscle length in um for each line ($P > 0.05$). (D) Contractility index results received from *in silico* simulation (E) Contractility index results received via 3 methods: Straight vertical line - CI calculated from mean of all data (without matching to pairs), dotted vertical line - CI calculated from median of all data (without matching to pairs) and histogram received from *in silico* simulation described in methods.

5.1.4 Muscle-specific Hsp67Bc silencing increases the level of muscle protein oxidation

Two repetitions of the Oxyblot experiment were performed, which are represented in Fig. 9. by two separated columns. Oxidation indexes calculated from membranes after immunodetection (Fig. 9C,D) normalized to Ponceau staining (Fig. 9A,B) are represented on plots (Fig. 9E,F). The median oxidation index in RNAi expressing line is 15% higher compared to the control group (Fig. 10). Differences between control and RNAi expressing line are not statistically significant because not enough repetitions of the Oxyblot experiment have been made.

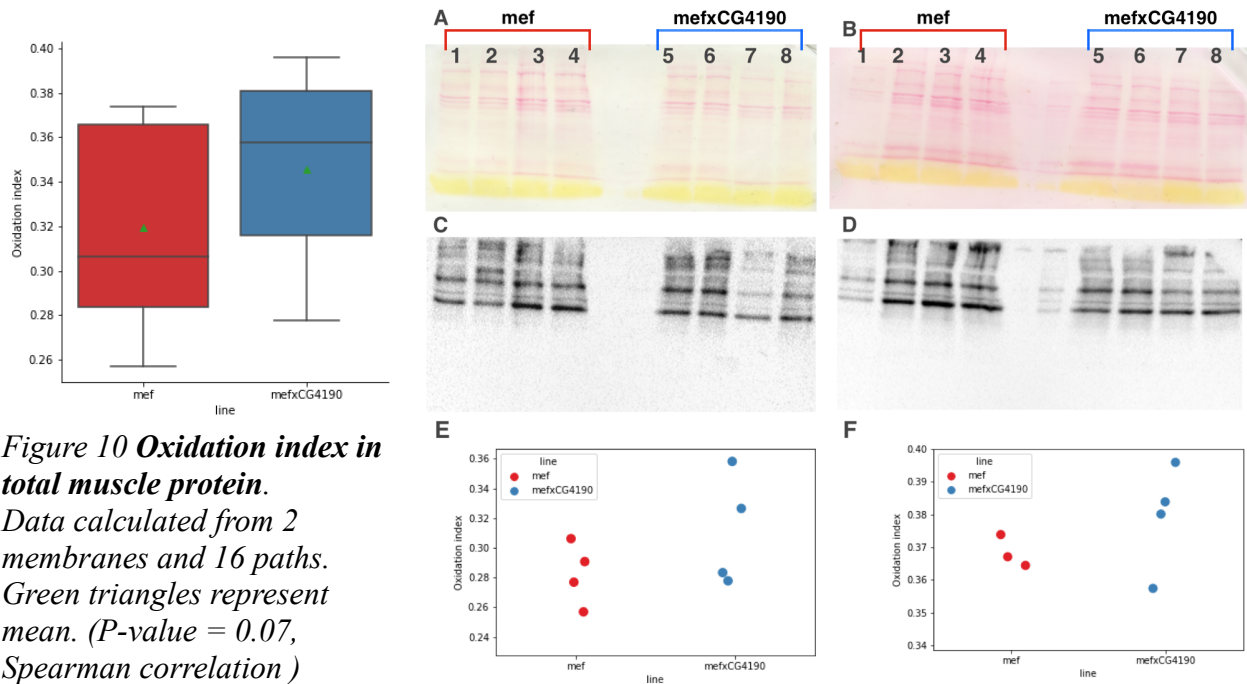


Figure 10 Oxidation index in total muscle protein.

Data calculated from 2 membranes and 16 paths. Green triangles represent mean. ($P\text{-value} = 0.07$, Spearman correlation)

Figure 9: Oxyblot with larvae body wall muscle with muscle-specific Hsp67Bc silencing.

Total protein from larvae muscle after derivatization process is transferred to nitrocellulose membranes. Each column of the figure represents repetition of the Oxyblot experiment. Each number of lane from 1 to 8 represents samples from the same lysates. (A,B) Membranes after Ponceau staining. (C, D) Membranes after detection and documentation (E, F) plots with oxidation indexes are calculated from each path.

5.2 Evaluation of neuronal-specific Hsp67Bc silencing

5.2.1 Neuronal-specific Hsp67Bc silencing alters NMJ structure

There are two statistically significant differences in NMJ morphology between the two examined lines. Mean radius of synaptic button is smaller in RNAi expressing line compared to control line ($P = 0.05$) (Fig. 11A) Additionally, the number of synaptic buttons is higher in RNAi expressing line compared to the control line. This difference

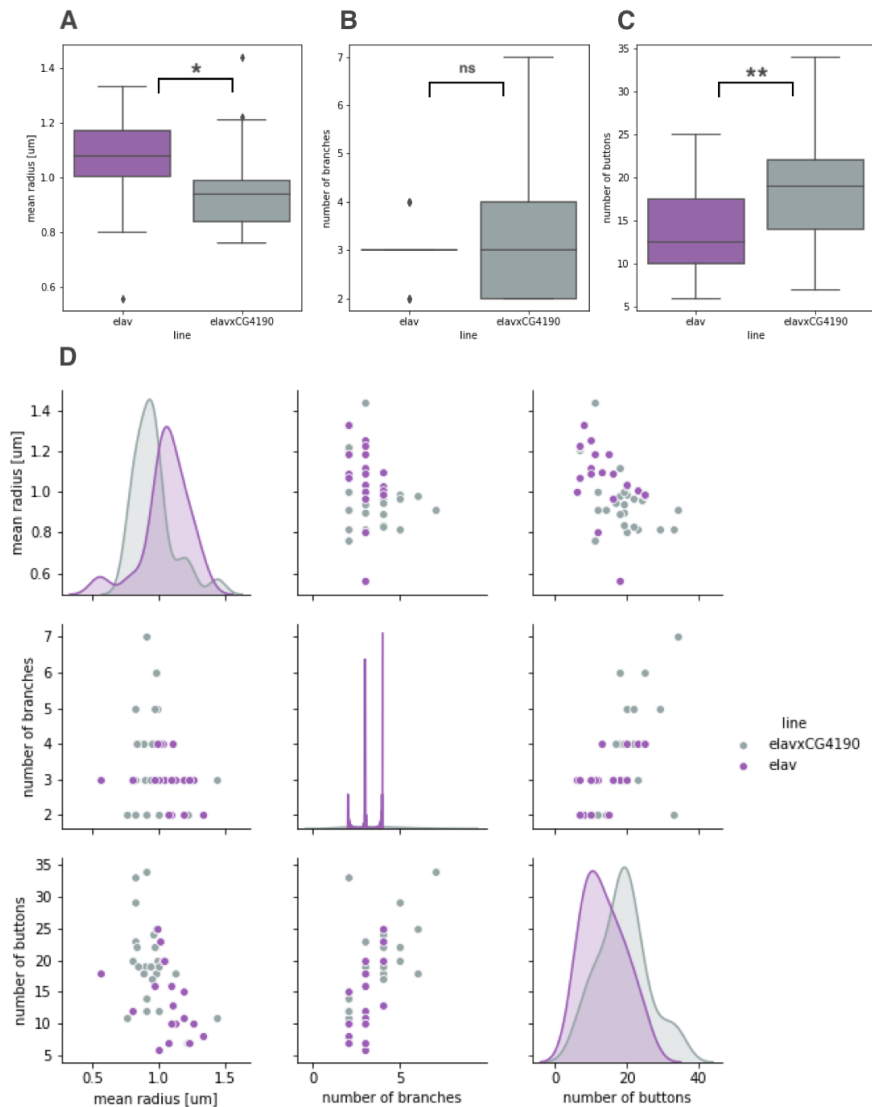


Figure 11: NMJ Morphometric measurements of larvae with nerve-specific Hsp67Bc silencing.

(A) Mean radius of synaptic buttons in LL1 muscle nerve. (B) Number of branches in LL1 muscle nerve. (C) Number of synaptic buttons in LL1 muscle nerve. (D) Correlations for each individual muscle nerve results between all NMJ experiments and distribution of datasets. $N=18$ for control and $n=24$ for RNAi expression line.

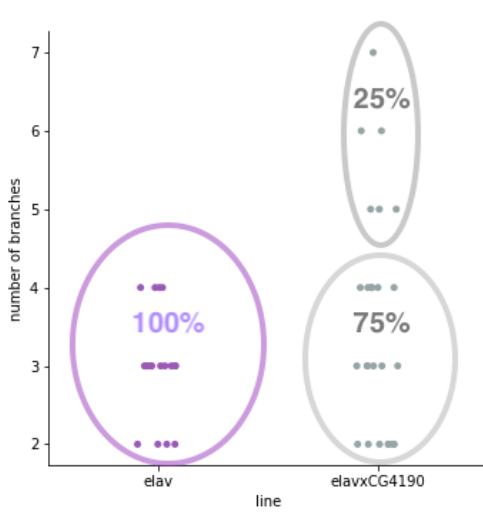


Figure 12: Number of branches with NMJ depending on line.

However a certain percentage of the RNAi expressing NMJ contained 5, 6, and 7 branches. This was not observed in control. Individuals with high number of branches represent 25 % of all RNAi expressing NMJ (Fig. 12)

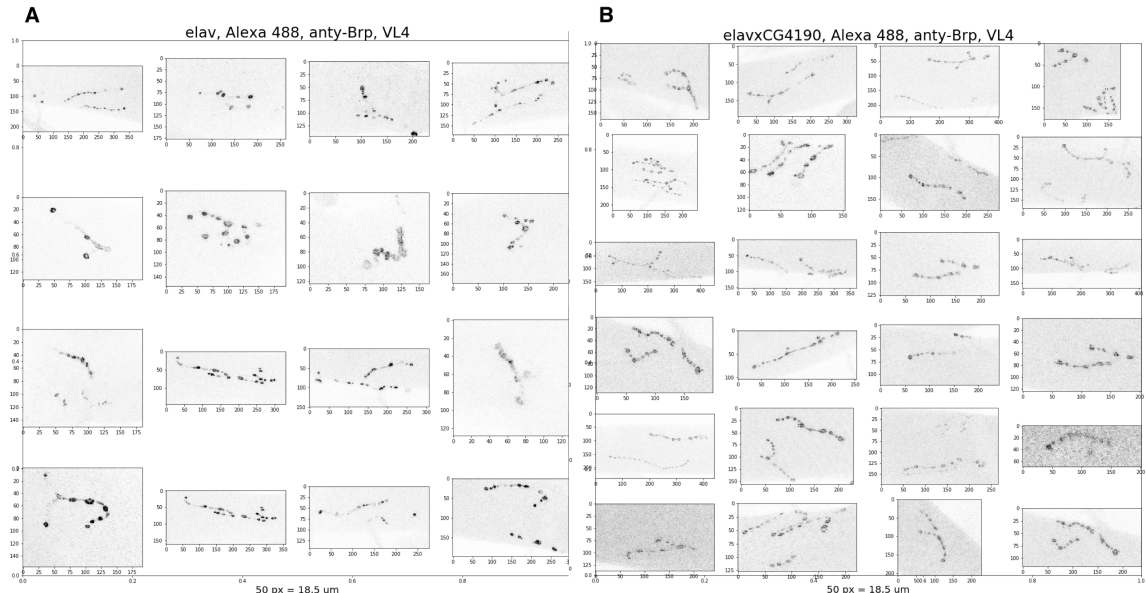


Figure 13: NMJ morphometric measurements: elav and elavxCG4190 lines.

Figure shows microscopy images with individual nerves on LL1 muscles, used to this study (only red channel with signal from anti-Brp antibody, converted to gray scale to better visibility). (A) Control line. (B) RNAi expressing line. Based on photographs taken by Ph.D. Magda-Dubińska Magiera

is also statistically significant ($P = 0.01$) (Fig. 11C). Data shows a linear relationship between mean radius and number of synaptic buttons for both lines: bigger radii of synaptic buttons coexists with a smaller number of them (Fig. 11D). RNAi line creates subset of LL1 muscles with a higher number of statistically small synaptic buttons. This trend is visible on the microscopy images (Fig. 13).

The statistically significant difference in a number of branches between control and RNAi expressing lines (Fig. 11B) is not observed.

5.2.2 Neuronal-specific Hsp67Bc silencing alters larva behavior in righting and crawling assay

For the experiment with Elav drivers four aspects of behavior were measured: crawling assay (number of peristaltic movements, reorientations points and distance in mm per 30 seconds) and righting assay. There were no statistically significant differences between control and RNAi line in a number of peristaltic movements per 30 seconds and crawling distance (Fig. 14A,D). In righting test time to come back to the normal position was significantly shorter ($P < 0.01$) in the control line (Fig. 14C). A number of reorientation points was significantly higher for RNAi expression line ($P < 0.0001$) (Fig. 14B).

Result of righting time is independent of any crawling experiment for each individual. There is ascending linear correlation between peristaltic movements per 30 s and crawling distance for both lines (but both experiments are not statistically significant). There is a linear descending correlation between a number of reorientation points and crawling distance for both lines. There is a small bimodal trend in RNAi expressing line in righting time and distance (Fig. 14E).

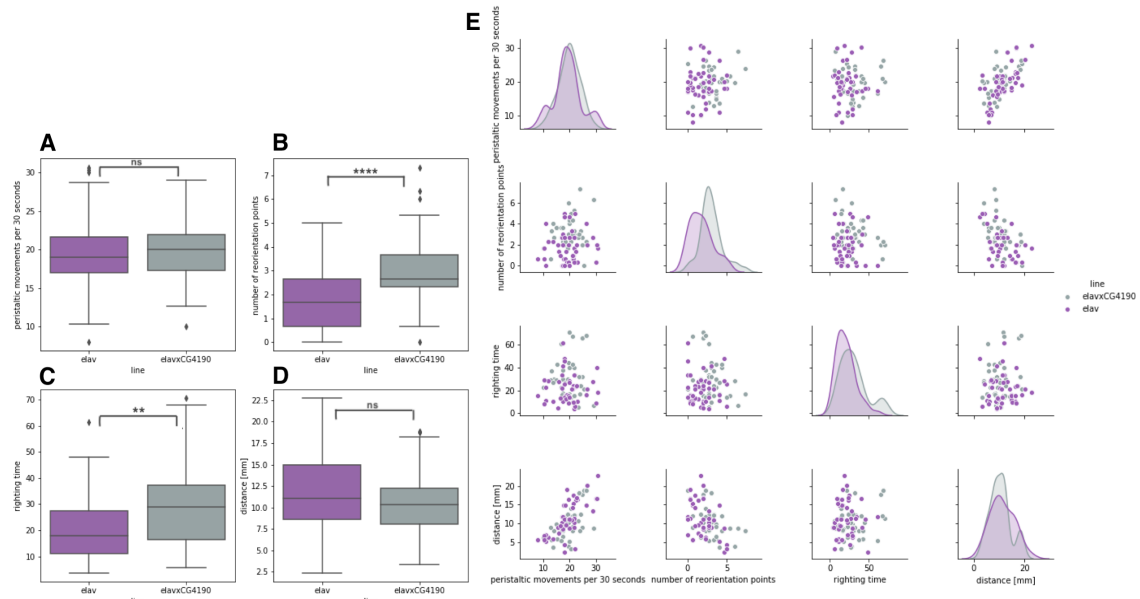


Figure 14: Behavioral tests of larvae with nerve-specific Hsp67Bc silencing.

Results of behavioral tests with 3rd instar larva using Elav-Gal4 driver line as control ($n=45$). Each larva was measured 3 times and mean was calculated. (A) number of peristaltic movements per 30 seconds ($P>0.05$), (B) number of reorientation points per 30 seconds ($P<0.0001$), (C) Righting assay – time in seconds to come back to normal body position ($P<0.01$). (D) distance in mm ($P>0.05$). (E) Correlation between crawling and righting assay for each individual and distribution of the datasets.

CHAPTER 6: DISCUSSION

Hsp67Bc is protein taking part in cell homeostasis in stress conditions. Hsp67Bc participate in *Drosophila melanogaster* development even in stress independent processes. It is a member of protein complex which takes part in Z and A band maintenance in skeletal muscles. Hsp67Bc is expressed in the most tissues which suggests its role in more biological processes that are related to muscle functioning. Its human ortholog HSPB8 is related to neurodegenerative diseases. Knowledge about the role of HSPB8 and cooperation with other proteins is a potential possibility to discover treatment to diseases related to HSPB8. *D. melanogaster* Hsp67Bc research give possibility to get knowledge easier, faster, less expensive and without ethical dilemmas in comparison to research on vertebrates. On another hand, *D. melanogaster* is not an organism closely related to human and not all of proteins have defined orthologs. Biological functions and interactions of ortholog proteins can be similar to mammals but not identical, which is a disadvantage. However, discoveries by studying orthologs can be a prelude to studies on higher organisms, more related to human.

Result of experiments performed in this master thesis shows that Hsp67Bc has important function in larva's organism. Its knock-down causes negative effects on tissue structure and behavior.

Results from behavioral tests on muscle-specific RNAi larvae are different than expected during the planning of experiments. There are discoveries about the important role of Hsp67Bc in the maintenance of Z and A-bands. Any abnormalities connected to its expression should lead to disruption of muscle function which in general leads to decrease in a number of peristaltic movements and longer righting time [13], [33]. Herein the result of righting tests is surprising, because organism with muscles with abnormalities such as fuzzy Z-bands, in theory should have longer righting time (Fig. 7). Even though larvae with muscle-specific RNAi expression have disrupted structure they have at the same time shorter righting time. It's difficult to find any explanation of this effect, but maybe knock-down has another effect on larvae behavior which is not known yet.

Muscle-specific knock-down explicitly leads to negative effect on muscle structure because most of the examined muscles – VL3 and VL4 have some abnormalities such as fuzzy Z-bands and splitted muscle fibers. Such abnormalities are also visible in the muscles located in the vicinity of VL3 and VL4 muscles. Assessment of muscle structure on the basis of microscopic images requires knowledge and experience in finding difference between real anatomical changes and artifacts resulted in the improper dissection procedure. The other difficulty in data interpretation is presence of abnormalities in control group. However, these abnormalities in control group are present in negligible percentage of individuals in comparison to the RNAi expression line (Fig.6E). It suggests that RNAi expression increases number of abnormalities in muscle structure.

Oxyblot results are as expected but doubtful. In theory protein oxidation in organism with decreased sHSP level should be higher, because sHSPs protect the cell against oxidation [7] but there is no evidence yet that Hsp67Bc participates in this process. Oxyblot results are statistically insignificant, because of not enough repetitions of experiment. Doubts are also aroused by the fact that the methodology of Oxyblot is not optimized yet. There is no experimentally proven information about the error of this method, which could give information if results are caused by biological reason or standard error of methodology. In theory, Oxyblot is quantitative method and results should be comparable by oxidation in percentage or as oxidation index used herein. In practice the Western blot method is multistep and each step produces some percentage of error because of not optimized methodology and the human factor. Errors are cumulated during each crucial step making this method only qualitative but no quantitative. Finally biological changes which occur in an organism can not be detected [19]. Another standardization method which can be applied is performing protein oxidation *in-vitro* in different concentrations of oxidative ingredient which can give knowledge about real detection level of the method.

Neuronal-specific Hsp67Bc interference alters larvas behavior which was visible during the first repetition of the experiment. It was manifested by frequent turning back during crawling. The methodology of behavioral tests had to be changed to apply it to represent the abnormal behavior of larvas using numbers that can be then statistically analyzed. Assessed parameters involved a number of reorientation points and crawling

distance. The experiment resulted in the observation of a statistically significant difference between control and RNAi expressing line. The changes comprise a higher number of reorientation points in RNAi expressing line compared to control. This can suggest altered larvas orientation. Longer righting time in RNAi expression line can be connected by longer reaction to stress condition.

NMJ morphometric measurements allowed to find a correlation between neuronal-specific RNAi expression and NMJ morphology. Hsp67Bc protein is known as highly related to *D. melanogaster* nervous system. Abnormalities such as smaller synaptic buttons' perimeters correspond with behavioral tests. The question is why there is a correlation between number of buttons and its size (Fig. 11D) *D. melanogaster* NMJ are very dynamic structures with high environmental dependent plasticity including changes in number of synaptic buttons [34]. It could be that there exists a mechanism that increases the number of synaptic buttons in order to compensate their small size caused by altered development.

Experiments performed herein have one disadvantage, which is lack of information about larvas sex. Commonly used practice in *D. melanogaster* research is dividing individuals to males and females during experiments on adults, because of sexual dimorphism [28], [30].

It was also discovered that expression of GAL4 has higher efficiency in males than females thus sex control in RNAi in *D. melanogaster* is very important to understand the results of the experiment [23]. The higher phenotype effect in males was also observed in sHSPs RNAi screening with actin driver study, but without higher efficiency of interference in males proven by RT-PCR. However to relative measurement of RNAi expression was used another stage of development than phenotyping [30]. Herein in righting test there are small bimodal trends in RNAi line in both *mef* and *elav* drivers (Fig. 7C and Fig. 14E) which can suggest that among the population there are some larvas than have stronger phenotype than others, but this effect is too small to consider it as meaningful. However, in the future research, it is possible to collect data about larvas sex in behavioral tests, placing larvas in multiwell plates and waiting to transformation to imago stadium to distinguish sex or by sex genotyping using PCR.

NMJ morphometric measurements are an example of experiments with sexual dimorphism observed in larvae in parameters related to NMJ size, such as NMJs area, number of NMJs and number of active zones [24]. Herein in an experiment with morphometric measurement, there is a small population of RNAi expressing muscles with stronger phenotype in number of branches (Fig. 12) However, there are no proves that this is caused by sex of individual, and number of branches is known as sex independent feature. There is also a lack of information about the individual origin of the muscle, to distinguish which muscles are from the same organism which could overthrow that hypothesis.

D. melanogaster knock-down using RNAi screening is a technique with lots of advantages among other techniques in reverse genetics. Stocks libraries allow to easily conduct RNAi research on at least 91% of *D. melanogaster* protein-coding genes. GAL4-UAS system allows to gene-specific and stage-specific interference. Researcher receives ready fly stocks and does not need to perform any genetic engineering which is time and cost consuming. In comparison to knock-out technique, knock-down allows avoiding lethal effect which occurs in conservative, crucial genes. Knock-out using random mutagenesis or point mutations provided by genetic engineering can cause unpredictable effects of misfolded protein, additionally to loose of function.

Despite advantages there are still remaining problems such as off-target effect and ineffective interference of RNAi. Off target effect on genes with high homology can be easily detected, but off-target effects on distant genes with fragmental homologies are unpredictable. There are no available perfect techniques to detect all off target effects [17]. Results obtained in the frame of this thesis can give the direction of future Hsp67Bc study but can not be considered as evidence – need to be supported by another study than RNAi screening.

After experiment performed by Bouhy and colleagues [3] where HSPB8 knock-out mice developed to adult age, without lethal effect there is a new hypothesis. Probably there is a possible perspective of knock-out of Hsp67Bc in *D. melanogaster*, without lethal effect and which could eliminate disadvantages of RNAi research.

Another thing to consider in RNAi screening is to check interference efficiency before experiments, using some techniques, for example, RNA-seq, RT-PCR or Selfie-

digital PCR [26]. If the results of experiments are negative there is a possibility that interference is not sufficient. However, RNAi stock used in this study (Hsp67BcRNAi-UAS) was used before on actin driver with 70% efficiency of Hsp67Bc expression reduction [30]. Additionally, GAL4 *mef* and *elav* drivers are recommended as strong drivers without any problems of expression related to developmental stage [17]. RNA-Seq and microarrays can be also good method to find genes associated with Hsp67Bc interference. Microarrays methodology allowed to discover the interaction between Pacman protein and Hsp67Bc [15].

Techniques mentioned above allow to find the efficiency of interference on mRNA level, but to check expression on protein level another experiment has to be performed – for example, Western Blot.

There are evidence that mice HSPB8 knock-out and hot-spot mutated Hsp67Bc alter ultrastructure of mitochondria in muscle tissues. For this reason, investigating the ultrastructure of muscles with tissue-specific Hsp67Bc gene interference is necessary. Expected results are altered structure of mitochondria and sarcomeres.

Hsp67Bc is the ortholog of human HSPB8, responsible for neurodegenerative diseases if is mutated in hot-spot place in the sequence. This HSPB8 substitution of one nucleotide in the gene causes two different diseases with different clinical symptoms, dependent on substitution which is particularly interesting for researchers. In experiments with knock-out and hot-spot mutations of HSPB8 in mice phenotype of hot-spot mutated organisms represents an animal model of CMT and dHMN disease, but knock-out phenotype is mild in behavioral tests and different in morphology and ultrastructure [3]. The hypothesis is that knock-down of Hspb67Bc should also have a milder and different effect than hot-spot mutated phenotypes, studied before [14].

RNAi screening used in this thesis, expanded by other techniques detecting proteins which cooperate with Hsp67Bc would allow to getting knowledge about Hsp67Bc protein partners and pathways. Finally more knowledge can lead to finding treatment targets in Parkinson's, Alzheimer's and Huntington diseases, related to accumulation of toxic, amyloid aggregates.

In summary research on the impact of Hsp67Bc interference on muscle and nerve system is worth to continue and can provide new discoveries and expand still lacking

knowledge about this protein. The main hypothesis of the thesis is confirmed with compatible results from different experiments.

CHAPTER 7: ACKNOWLEDGMENTS

I would like to express my gratitude to my Supervisor - Magda Dubińska-Magiera for her patience and all didactical and technical support during the project.

Also, I would like to offer my special thanks for technical assistance in experiments and lab work to all researchers and technical staff from Department of Animal Developmental Biology, particularly to Ph.D's: Damian Lewandowski, Joanna Niedbalska-Tarnowska, Arnold Garbiewicz and Marta Migocka-Patrzałek.

My grateful thanks are also extended to lic. Tomasz Sobczak for his practical help and sharing experience and knowledge during the Oxyblot experiment.

Finally, I wish to thank the Student's Science Association "Programming Biologists" for support and help with statistics, data analysis and data visualization.

CHAPTER 8: LITERATURE

1. Armbruster, D. A. & Pry, T. *Limit of Blank, Limit of Detection and Limit of Quantitation*. *Clin Biochem Rev* **29**, (2008).
2. Ayme1, A. & Tissieres, A. *Locus 67B of Drosophila melanogaster contains seven, not four, closely related heat shock genes*. *ENIBO Journal* **4**, (1985).
3. Bouhy, D. *et al.* A knock-in/knock-out mouse model of HSPB8-associated distal hereditary motor neuropathy and myopathy reveals toxic gain-of-function of mutant Hspb8. *Acta Neuropathol.* (2018). doi:10.1007/s00401-017-1756-0
4. Carra, S. *et al.* Identification of the Drosophila ortholog of HSPB8: Implication of HSPB8 loss of function in protein folding diseases. *J. Biol. Chem.* **285**, 37811–37822 (2010).
5. Crippa, V. *et al.* The chaperone HSPB8 reduces the accumulation of truncated TDP-43 species in cells and protects against TDP-43-mediated toxicity. *Hum. Mol. Genet.* (2016). doi:10.1093/hmg/ddw232
6. Depre, C. *et al.* H11 kinase is a novel mediator of myocardial hypertrophy in vivo. *Circ. Res.* **91**, 1007–1014 (2002).
7. Dubińska-Magiera, M. *et al.* Contribution of small heat shock proteins to muscle development and function. *FEBS Letters* **588**, 517–530 (2014).
8. Escobedo, J., Pucci, A. M. & Koh, T. J. HSP25 protects skeletal muscle cells against oxidative stress. *Free Radic. Biol. Med.* **37**, 1455–1462 (2004).
9. Günther, M. N., Nettesheim, G. & Shubeita, G. T. Quantifying and predicting Drosophila larvae crawling phenotypes. *Sci. Rep.* (2016). doi:10.1038/srep27972
10. Haslbeck, M. *sHsps and their role in the chaperone network*. *CMLS, Cell. Mol. Life Sci* **59**, (2002).
11. Irobi, J. *et al.* Mutant HSPB8 causes motor neuron-specific neurite degeneration. *Hum. Mol. Genet.* (2010). doi:10.1093/hmg/ddq234
12. Irobi, J. *et al.* Hot-spot residue in small heat-shock protein 22 causes distal motor neuropathy. *Nat. Genet.* (2004). doi:10.1038/ng1328
13. Jabłońska, J., Dubińska-Magiera, M., Jagla, T., Jagla, K. & Daczewska, M. Drosophila Hsp67Bc hot-spot variants alter muscle structure and function. *Cell. Mol. Life Sci.* (2018). doi:10.1007/s00018-018-2875-z

14. Jabłońska, J., Dubińska-Magiera, M., Jagla, T., Krzysztof Jagla, · & Daczewska, M. Drosophila Hsp67Bc hot-spot variants alter muscle structure and function. *Cell. Mol. Life Sci.* **1**, 3 (2018).
15. Jones, C. I. *et al.* The 5'-3' exoribonuclease Pacman (Xrn1) regulates expression of the heat shock protein Hsp67Bc and the microRNA miR-277-3p in Drosophila wing imaginal discs. *RNA Biol.* **10**, 1345–1355 (2013).
16. Juneja, M., Burns, J., Saporta, M. A. & Timmerman, V. Challenges in modelling the Charcot-Marie-Tooth neuropathies for therapy development. *Journal of Neurology, Neurosurgery and Psychiatry* (2018). doi:10.1136/jnnp-2018-318834
17. Kaya-Çopur, A. & Schnorrer, F. A guide to genome-wide in vivo RNAi applications in drosophila. in *Methods in Molecular Biology* **1478**, 117–143 (Humana Press Inc., 2016).
18. Michaud, S., Marin, R. & Tanguay, R. M. Regulation of heat shock gene induction and expression during Drosophila development. *Cellular and Molecular Life Sciences* **53**, 104–113 (1997).
19. Mishra, M., Tiwari, S. & Gomes, A. V. Protein purification and analysis: Next generation western blotting techniques. *Expert Review of Proteomics* **14**, 1037–1053 (2017).
20. Morton, J. P., Kayani, A. C., McArdle, A. & Drust, B. The Exercise-Induced stress response of skeletal muscle, with specific emphasis on humans. *Sports Medicine* **39**, 643–662 (2009).
21. Mymrikov, E. V., Seit-Nebi, A. S. & Gusev, N. B. Large Potentials of Small Heat Shock Proteins. *Physiol. Rev.* (2011). doi:10.1152/physrev.00023.2010
22. Naidoo, N., Ferber, M., Master, M., Zhu, Y. & Pack, A. I. Aging Impairs the Unfolded Protein Response to Sleep Deprivation and Leads to Proapoptotic Signaling. *J. Neurosci.* **28**, 6539–6548 (2008).
23. Ni, J. Q. *et al.* Vector and parameters for targeted transgenic RNA interference in Drosophila melanogaster. *Nat. Methods* **5**, 49–51 (2008).
24. Nijhof, B. *et al.* A New Fiji-Based Algorithm That Systematically Quantifies Nine Synaptic Parameters Provides Insights into Drosophila NMJ Morphometry. *PLoS Comput. Biol.* **12**, (2016).
25. Pauli, D. & Tonka, C. H. A Drosophila heat shock gene from locus 67B is expressed during embryogenesis and pupation. *J. Mol. Biol.* (1987). doi:10.1016/0022-2836(87)90309-3

26. Podlesniy, P. & Trullas, R. Absolute measurement of gene transcripts with Selfie-digital PCR. *Sci. Rep.* **7**, (2017).
27. Qiu, H. *et al.* H11 kinase/heat shock protein 22 deletion impairs both nuclear and mitochondrial functions of stat3 and accelerates the transition into heart failure on cardiac overload. *Circulation* **124**, 406–415 (2011).
28. Rybina, O. Y. *et al.* Tissue-specific transcription of the neuronal gene Lim3 affects *Drosophila melanogaster* lifespan and locomotion. *Biogerontology* **18**, 739–757 (2017).
29. Sun, X. *et al.* Interaction of Human HSP22 (HSPB8) with Other Small Heat Shock Proteins. *J. Biol. Chem.* **279**, 2394–2402 (2004).
30. Takahashi, K. H., Rako, L., Takano-Shimizu, T., Hoffmann, A. A. & Lee, S. F. Effects of small Hsp genes on developmental stability and microenvironmental canalization. *BMC Evol. Biol.* (2010). doi:10.1186/1471-2148-10-284
31. Vicario, M., Skaper, S. & Negro, A. The Small Heat Shock Protein HspB8: Role in Nervous System Physiology and Pathology. *CNS Neurol. Disord. - Drug Targets* **13**, 885–895 (2014).
32. Vos, M. J. *et al.* Specific protein homeostatic functions of small heat-shock proteins increase lifespan. *Aging Cell* (2016). doi:10.1111/acel.12422
33. Wojtowicz, I. *et al.* Drosophila small heat shock protein CryAB ensures structural integrity of developing muscles, and proper muscle and heart performance. *Development* (2015). doi:10.1242/dev.115352
34. Yeates, C. J., Zwiefelhofer, D. J. & Frank, C. A. The Maintenance of Synaptic Homeostasis at the Drosophila Neuromuscular Junction Is Reversible and Sensitive to High Temperature . *eneuro* **4**, ENEURO.0220-17.2017 (2017).

CHAPTER 9: ABSTRACT

9.1 Streszczenie w języku polskim (abstract in Polish language)

Gen Hsp67Bc koduje białko Hsp67Bc, które należy do rodziny małych białek szoku cieplnego. Białko to zapobiega powstawaniu toksycznych agregatów innych białek i odpowiada za utrzymanie homeostazy komórki. Badania RNA-seq wykazały że białko to jest ekspresjonowane na różnym poziomie we wszystkich przebadanych narządach i układach. Ponadto zauważono że lokalizuje się w prążkach linii Z i A sarkomerów mięśni oraz w połączeniach nerwowo-mięśniowych, co prawdopodobnie świadczy o jego udziale w utrzymaniu ich prawidłowej struktury. W niniejszej pracy zastosowano specyficzne-tkankowo wyciszenie genu Hsp67Bc u larw *D. melanogaster* w celu lepszego poznania roli tego białka. Wyciszenie specyficzne mięśniowo prowadziło do zaburzeń behawioralnych larw, nieprawidłowej struktury mięśni somatycznych oraz nieznacznie podwyższzonego poziomu oksydacji białek mięśniowych, natomiast wyciszenie specyficzne dla układu nerwowego prowadziło zarówno do zaburzeń behawioru, zmienionej liczby i wielkości kolbek synaptycznych.

9.2 Abstract in English language

Hsp67Bc gene codes Hsp67Bc protein, which is a member of Small Heat Shock Proteins family. Hsp67Bc protects cells against toxic protein aggregation and is responsible for cell homeostasis. RNA-seq studies show that this protein is expressed at different levels in most of the *Drosophila melanogaster* tissues and organs. Moreover other studies show its Z and A-band and NMJs localization, which suggests its role in the maintenance of their proper structure. In this thesis tissue-specific Hsp67Bc interference in *D. melanogaster* larvae has been applied to get better knowledge about the role of the Hsp67Bc. Muscle-specific knock-down leads to behavioral changes, improper muscle structure and a higher level of muscle proteins oxidation. Knock-down in the nervous system leads to behavioral changes and different number and size of neuromuscular buttons.